ELSEVIER

Biophysical Chemistry 93 (2001) 171–179

Biophysical Chemistry

www.elsevier.com/locate/bpc

A unified picture of protein hydration: prediction of hydrodynamic properties from known structures

Huan-Xiang Zhou*

Department of Physics, Drexel University, Philadelphia, PA 19104, USA

Received 13 February 2001; received in revised form 17 July 2001; accepted 18 July 2001

Abstract

Hydration is essential for the structural and functional integrity of globular proteins. How much hydration water is required for that integrity? A number of techniques such as X-ray diffraction, nuclear magnetic resonance (NMR) spectroscopy, calorimety, infrared spectroscopy, and molecular dynamics (MD) simulations indicate that the hydration level is 0.3–0.5 g of water per gram of protein for medium sized proteins. Hydrodynamic properties, when accounted for by modeling proteins as ellipsoids, appear to give a wide range of hydration levels. In this paper we describe an alternative numerical technique for hydrodynamic calculations that takes account of the detailed protein structures. This is made possible by relating hydrodynamic properties (translational and rotational diffusion constants and intrinsic viscosity) to electrostatic properties (capacitance and polarizability). We show that the use of detailed protein structures in predicting hydrodynamic properties leads to hydration levels in agreement with other techniques. A unified picture of protein hydration emerges. There are preferred hydration sites around a protein surface. These sites are occupied nearly all the time, but by different water molecules at different times. Thus, though a given water molecule may have a very short residence time ($\sim$ 100–500 ps from NMR spectroscopy and MD simulations) in a particular site, the site appears fully occupied in experiments in which time-averaged properties are measured.

Keywords: Hydration; Hydration sites; Residence time; Diffusion constant; Intrinsic viscosity; Rotational correlation time

1. Introduction

Hydrodynamic measurements are one of the oldest techniques for characterizing the size and shape of protein molecules. Historically molecular dimensions were estimated from the expressions of hydrodynamic properties for ellipsoids [1–4]. Owing to the crudeness of ellipsoids as models of globular proteins, hydrodynamic hydration levels have varied widely, from 0.1 to over 1.0 g of water per gram of protein. Now several numerical techniques based on modeling the de-

* Tel.: +1-215-895-2716; fax: +1-215-895-5934.
E-mail address: hxzhou@einstein.drexel.edu (H.-X. Zhou).

0301-4622/01/$ - see front matter
PII: S0301-4622(01)00219-8

tailed structures of proteins have been developed to calculate hydrodynamic properties [5–8]. It is time to re-examine the issue of hydrodynamic hydration.

A number of techniques such as X-ray diffraction, nuclear magnetic resonance (NMR) spectroscopy, calorimety, infrared spectroscopy, and molecular dynamics simulations indicate that the hydration level is 0.3–0.5 g of water per gram of protein for medium sized proteins. For example, a recent high-resolution X-ray diffraction of ribonuclease A identified 258 water molecules in the first hydration shell [9], corresponding to a hydration level of 0.34 g/g. The non-freezable water around a protein can be easily detected by NMR. The hydration levels from such a measurement are 0.34, 0.42 and 0.34 g/g for lysozyme, myoglobin, and chymotrypsinogen A, respectively [10]. Calorimetric measurements of the heat capacity of lysozyme powder at different hydration levels indicate that the amount of water required to hydrate lysozyme is 0.38 g/g (i.e. any additional water beyond this hydration level simply becomes part of the bulk water) [11]. Similarly, infrared spectroscopy indicates that hydration of lysozyme stops at approximately 0.33 g/g [12–14]. Molecular dynamics simulations of myoglobin solvated by different numbers of water molecules show that root-mean-square deviations from the X-ray structure become stable after approximately 350 water molecules (i.e. 0.37 g/g) are included [15].

In earlier work we presented hydrodynamic calculation results to indicate that when the detailed structures of proteins are explicitly modeled, hydration levels in the narrow range of 0.3–0.5 g/g are predicted [7]. Here we present additional data on rotational correlation times to support this conclusion.

2. Relations of hydrodynamic and electrostatic properties

The connection between hydrodynamic and electrostatic properties was recognized from the fact that the Oseen Tensor, i.e. the Green function for the Navier–Stokes equation, when orientationally averaged is proportion to the Green function for the Laplace equation [16]. One has

$$\tilde{T} = \frac{1}{8\pi\eta_0 R}(\tilde{I} + \hat{\mathbf{R}}\hat{\mathbf{R}}) \tag{1a}$$

$$\langle \tilde{T} \rangle_0 = \frac{1}{6\pi\eta_0 R}\tilde{I} = \frac{2}{3\eta_0}\gamma(\mathbf{R})\tilde{I} \tag{1b}$$

where $\mathbf{R} = R\hat{\mathbf{R}} = \mathbf{r}' - \mathbf{r}$,$\tilde{\mathbf{I}}$ is the identity tensor, η_0 is the viscosity of the fluid, $\langle \ldots \rangle_0$ denotes averaging over a uniform distribution of orientations, and

$$\gamma(\mathbf{R}) = \frac{1}{4\pi R} = \frac{1}{4\pi|\mathbf{r}' - \mathbf{r}|} \tag{2}$$

By approximating the Oseen tensor by its orientational average, Zhou [16] showed that the translational friction is related to the electric capacitance by

$$\xi = 6\pi\eta_0 C \tag{3}$$

In particular this result is exact for triaxial ellipsoids. By the same approximation, the intrinsic viscosity is proportional to the electric polarizability. To make the relation exact for a sphere, Zhou proposed adding a term proportional to the volume of particle under consideration. Thus we have

$$[\eta] = \frac{3}{4}\alpha + \frac{1}{4}V_{\mathrm{p}} \tag{4}$$

The capacitance is the total charge on the surface of the particle if it were a conductor with the surface electric potential maintained at unity. That is,

$$C = \int_{S_{\mathrm{p}}} \mathrm{d}s\sigma_c(\mathbf{r}) \tag{5a}$$

$$4\pi\int_{S_{\mathrm{p}}} \mathrm{d}s\gamma(\mathbf{r} - \mathbf{r}')\sigma_{\mathrm{c}}(\mathbf{r}) = 1 \tag{5b}$$

where S_{p} is the surface of the particle and $\sigma_{\mathrm{c}}(\mathbf{r})$ is

the surface charge density. The electric polarizability tensor $\tilde{\alpha}$ has the components

$$\alpha_{ij} = 4\pi \int_{S_p} ds x_i \sigma_j(\mathbf{r}) \tag{6}$$

where x_i are the Cartesian components of $\mathbf{r}$, and $\sigma_j(\mathbf{r})$ are the charge densities satisfying

$$4\pi \int_{S_p} ds \gamma(\mathbf{r}-\mathbf{r}')\sigma_j(\mathbf{r}) = x_j' \tag{7}$$

The origin for the coordinate system should be chosen such that the total charges $\int_{S_p} ds \sigma_j(\mathbf{r})$ are zero. In practice, one can choose any origin and calculate $\sigma_j(\mathbf{r})$ according to Eq. (7). If the total charges are $\int_{S_P} ds \sigma_j(\mathbf{r}) = Q_j$, then the charge densities to be used for calculating the polarizability tensor should be $\sigma_j(\mathbf{r}) - (Q_j/C)\sigma_c(\mathbf{r})$. The orientationally averaged polarizability is

$$\alpha = \frac{1}{3}\sum_{i=1}^{3} \alpha_{ii} = Tr(\tilde{\alpha})/3 \tag{8}$$

By the orientational average of the Oseen tensor, Zhou [16] also showed a relationship between the rotational friction tensor $\tilde{\zeta}$ and the polarizability tensor. This is given by

$$\tilde{\zeta} = 3\eta_0(3\alpha \tilde{I} - \tilde{\alpha})/2 \quad \equiv 3\eta_0 \tilde{\beta} \tag{9}$$

The accuracy of this relation was not as extensively tested as that of Eqs. (3) and (4). In the case of an axially symmetric particle, Zhou did conjecture a relation between the axial rotational friction and the transverse electric polarizability. This is

$$\xi_{\parallel} = 2\eta_0 \alpha_{\perp} \tag{10}$$

which is proven in Appendix A. For axisymmetric particles, Eq. (9) predicts $\zeta_{\parallel} = 3\eta_0\alpha_{\perp}$ and $\zeta_{\perp} = 3\eta_0(\alpha_{\parallel} + \alpha_{\perp})/2$. The former differs from the exact result in Eq. (10) by a coefficient of 3 instead of 2. For ellipsoids, cylinders, and dumbbells, the proportionality constant between $\zeta_{\perp}$ and $\eta_0(\alpha_{\parallel} + \alpha_{\perp})/2$ was found to range from 2 for shapes close to a sphere to 4 for needles and disks.

The translational diffusion constant is related to the translational friction via the Stokes–Einstein equation

$$D = k_B T/\xi \tag{11}$$

where $k_B T$ is the product of the Boltzmann constant and the absolute temperature. A similar equation relates the rotational diffusion tensor $\tilde{D}^r$ and the rotational friction tensor. Globular proteins have traditionally been modeled as isotropic diffusers. More recently in interpreting NMR relaxation data on backbone dynamics proteins have been modeled as axisymmetric diffusers, with $D_{\parallel}/D_{\perp} = \zeta_{\perp}/\zeta_{\parallel}$ ranging from 0.8 to 1.4 [17–24]. The rotational correlation function of a unit vector attached to the particle is [25] is

$$C(t) = (1.5\cos^2\theta - 0.5)^2 e^{-t/t_1} + 3\sin^2\theta\cos^2\theta e^{-t/t_2} + 0.75\sin^4\theta e^{-t/t_3} \tag{12}$$

where θ is the angle between the unit vector and the symmetric axis, $1/t_1 = 6D_{\perp} = 6k_B T/\zeta_{\perp}$, $1/t_2 = 5D_{\perp} + D_{\parallel} = k_B T(5/\zeta_{\perp} + 1/\zeta_{\parallel})$, and $1/t_3 = 2D_{\perp} + 4D_{\parallel} = k_B T(2/\zeta_{\perp} + 4/\zeta_{\parallel})$. For $0.8 < D_{\parallel}/D_{\perp} = \zeta_{\perp}/\zeta_{\parallel} < 1.4$, Eq. (12) is well approximated by a single exponential. In Fig. 1 we compare Eq. (12) at $D_{\parallel}/D_{\perp} = 1.2$ against the single exponential function $\exp(-t/t_c)$ with an effective correlation function

$$t_c = (2\zeta_{\perp} + \zeta_{\parallel})/18k_B T \quad = Tr(\tilde{\zeta})/18k_B T \tag{13}$$

The agreement is very reasonable, with the area under the curve overestimated by 6.7% at $\theta = 0$ and underestimated by 2.5% at $\theta = 90°$ by the single-exponential function. Comparable amounts of errors are incurred at $D_{\parallel}/D_{\perp} = 0.8$.

Note that the rotational correlation time in Eq. (13) is not defined in the usual way as $t_c = 1/2(2D_{\perp} + D_{\parallel}) = 1/2k_B T(2/\zeta_{\perp} + 1/\zeta_{\parallel})$. The

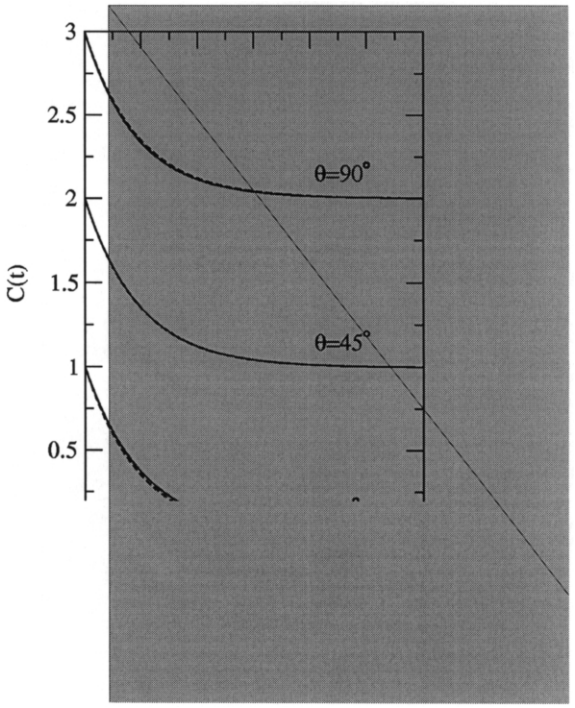

Fig. 1. Rotational correlation function of a unit vector attached to a axisymmetric diffuser. Solid curves are the exact result given by Eq. (12) and dashed ones are single-exponential approximations with correlation time given by Eq. (13). The curves for $\theta = 45$ and 90° are shifted upward by 1 and 2, respectively. Note that for $\theta = 45°$ the two curves are barely distinguishable.

result in Eq. (13) is larger by approximately 1% at $D_{\parallel}/D_{\perp} = 1.2$ and 0.8. The reason for using Eq. (13) is that we want to relate t_c to the orientationally averaged electric polarizability [see Eqs. (9) and (8)]. Considering the small deviations of $D_{\parallel}/D_{\perp}$ from 1 observed on globular proteins, we propose the following relation

$$t_c = 2.3\eta_0\alpha/6k_BT \quad (14)$$

The numerical factor, 2.3, is between the value 2 for a sphere and 3 according to Eq. (9).

Eq. (14) is the main theoretical result of the present paper. Along with the previously proposed Eqs. (3) and (4), we can now obtain the translation diffusion constant, the intrinsic viscosity, and the rotational correlation time simultaneously from a single electrostatic calculation for the capacitance and the polarizability. The details of this calculation are described previously [7]. In the next section we present results on the hydrodynamic properties of proteins predicted on their actual structures.

3. Results

Zhou [7] has used Eqs. (3) and (4) to calculate the translational diffusion constant and the intrinsic viscosity for ribonuclease A, lysozyme, myoglobin, and chymotrypsinogen A. By including a 0.9-Å-thick uniform hydration shell, the experimental results for both hydrodynamic properties are reproduced for all four proteins. Table 1 gives the comparison (data taken from Zhou [7]). The 0.9-Å-thick uniform hydration shell gives hydration levels of 0.40, 0.39, 0.40, 0.38 g of water per gram of protein for the four proteins.

The same calculation results contain other data that can be directly compared with experiments. In Table 2 we compare the volume V_p enclosed by the shell 0.9 Å away from the van der Waals surface of the protein with the hydrated volume as determined by small-angle X-ray scattering. Kumosinski and Pessen [26] compiled data for 18 proteins, among which are ribonuclease A, lysozyme, and chymotrypsynogen A. The values of V_p used for predicting D and $[\eta]$ agree with the experimental data on the hydrated volume to within 5, 10 and 4%, respectively, for the three proteins.

With Eq. (14) proposed in the present paper, we can now predict the rotational correlation time. The results, by using the previously calculated polarizablility [7] (listed in Table 1) in Eq. (14), are shown in Table 3. The predicted values of t_c are consistent with experimental results for all four proteins.

4. Discussion

With Eqs. (3), (4) and (14), we now have com-

Table 1
Electrostatic and hydrodynamic properties (at 20°C) of four proteins

Proteins	V_p (Å^3)	C (Å)	α (Å^3)	D (10^{-7} cm^2/s)		[η] (cm^3/g)		Hydration (g/g)
				Calculation	Experiment	Calculation	Experiment	
Ribonuclease A	20.941	19.24	91.691	11.06	11.2 ± 0.2	3.26	3.30 ± 0.04	0.40
Lysozyme	21.668	19.03	87.640	11.18	11.2 ± 0.2	2.99	2.99 ± 0.01	0.39
Myoglobin	27.631	20.52	110.288	10.37	10.3	3.14	3.15	0.40
Chymotrypsinogen A	39.190	23.06	153.540	9.23	9.2 ± 0.2	2.93	2.82 ± 0.3	0.38

Table 2
Comparison of modeled and experimental hydrated volumes (Å^3)

Proteins	Model	Experiment
Ribonuclease A	20 941	22 000
Lysozyme	21 668	24 200
Chymotrypsinogen A	39 190	37 790

Table 3
Comparison of predicted and experimental rotational correlation times (ns) at 20°C

Proteins	Prediction	Experiment
Ribonuclease A	8.8	8.3[a]
Lysozyme	8.4	7.2[b] 7.5[c] 10[d]
Myoglobin	10.5	8.9[e], 9.4[f] 12.7[g]
Chymotrypsinogen A	14.7	15[h]

[a] Converted from the result of 7.3 ns at 25°C in Krause and O'Konski [27].
[b] Cross and Fleming [28].
[c] Dill and Allerhand [29].
[d] Bubin et al. [30].
[e] Converted from the result of 10.3 ns at 15°C in Anderson et al. [31].
[f] Tao [32].
[g] Calculated from the steady-state fluorescence data of Stryer [33] by using a fluorescence lifetime of 16.4 ns for ANS complexed to apomyoglobin, as measured in Anderson et al. [31] and Tao [32].
[h] Stryer [34].

pleted an approach to predict the three hydrodynamic properties, translational diffusion constant, intrinsic viscosity, and rotational correlation time, of globular proteins, without any adjustable parameters. The new data in Tables 2 and 3 demonstrate the accuracy of our approach.

A very important physical property that come out of the hydrodynamic calculations is the hydration level. This falls within the narrow range of 0.3–0.5 g of water per gram of protein for all the

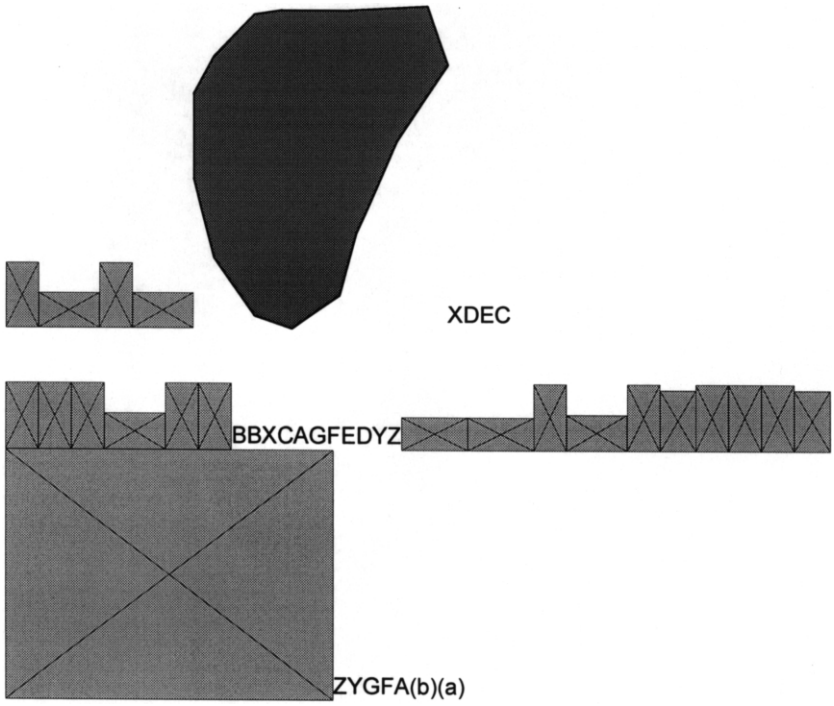

Fig. 2. The model of protein hydration. The protein is represented by the shaded area. Hydration water molecules have a black dot, whereas bulk water molecules have an open circle. (a) and (b) represent two time instances. In (a) water molecules A–G hydrate the protein and X–Z are in the bulk. In (b) the protein has undergone a rotation (and translation), and the sites initially occupied by molecules A, B, and C are now occupied by X, Y, and Z, respectively. Note that the hydration sites around the protein are fixed, even a given site may be occupied by different water molecules at different times.

four proteins considered in this paper. By using the detailed protein structures, we have brought the hydration levels implicated by hydrodynamic properties into conformity with those detected by other experimental techniques.

It now appears reasonable to propose a unified picture of protein hydration that reconciles observations from different experimental techniques. As Fig. 2 illustrates, around the protein surface are preferred hydration sites. As seen by X-ray diffraction and in molecular dynamics simulations, these sites are around charged side chains and polar side chains and the backbone, where water molecules can make hydrogen bonds with the protein. Though a given water molecule may have a residence time of only 100–500 ps in a particular site (as determined by NMR spectroscopy [35]), the site is almost fully occupied (albeit by different water molecules at different times). Thus, in experiments (e.g. calorimetry and hydrodynamic measurements) which detect time-averaged properties the hydration water appears as an integral part of the protein. It is important to note that hydration water is marked by the permanence of the occupation sites, not by the permanence of the occupants.

Appendix A

In this appendix we prove Eq. (10), the exact result relating the axial rotational friction and the transverse electric polarizability of an axially symmetric particle.

For a fluid perturbed by the axial rotation of an axisymmetric particle, the only non-zero component of the fluid velocity is in the azimuthal direction. This we will denote as v. In cylindrical coordinates the Navier–Stokes equation for v is [36]

$$\frac{1}{\rho}\frac{\partial}{\partial\rho}\left(\rho\frac{\partial v}{\partial\rho}\right)+\frac{\partial^2 v}{\partial z^2}-\frac{v}{\rho^2}=0 \tag{A1}$$

The boundary conditions are

$$v|_{S_p}=\Omega\rho \tag{A2a}$$

$$v\left(\sqrt{\rho^2+z^2}\to\infty\right)=0 \tag{A2b}$$

where S_p is the surface of the particle and Ω is the rotational velocity. By the transformation [37,38]

$$V=v\cos\phi \tag{A3}$$

Eq. (A1) can be converted to a Laplace equation

$$\nabla^2 V=0 \tag{A4}$$

The boundary conditions are now

$$V|_{S_p}=\Omega\rho\cos\phi \tag{A5a}$$

$$V\left(\sqrt{\rho^2+z^2}\to\infty\right)=0 \tag{A5b}$$

The surface stress force in the present case is [36]

$$\mathbf{f}=\mathbf{n}\cdot\tilde{\Pi}=-p\mathbf{n}+\eta_0\mathbf{n}\rho\nabla(v/\rho) \tag{A6}$$

The axial component of the resulting torque is

$$L=\int_{S_p}\mathrm{d}s(\mathbf{r}\times\mathbf{f})\cdot\hat{\mathbf{z}}=\eta_0\int_{S_p}\mathrm{d}s\mathbf{n}\cdot\rho^2\nabla(v/\rho) \tag{A7}$$

The axial rotational friction is

$$\zeta_{\|}=-L/\Omega\ =-\eta_0\int_{S_p}\mathrm{d}s\mathbf{n}\cdot\rho^2\nabla(v/\rho\Omega) \tag{A8}$$

The electrostatic potential φ induced by a uniform electric field, $E\hat{\mathbf{x}}$, in the transverse direction satisfies the Laplace equation

$$\nabla^2\varphi=0 \tag{A9}$$

with the boundary conditions

$$\varphi|_{S_p}=Ex=E\rho\cos\phi \tag{A10a}$$

$$\varphi\left(\sqrt{\rho^2+z^2}\to\infty\right)=0 \tag{A10b}$$

Comparing with Eqs. (4), (5a) and (5b) gives

$$\varphi = (E/\Omega)V = (E/\Omega)v\cos\phi \qquad \text{(A11)}$$

The transverse electric polarizability is [16]

$$\alpha_{\perp} = \int_{S_p} \mathrm{d}s\mathbf{n}\cdot(-\nabla\varphi + E\hat{\mathbf{x}})/E \qquad \text{(A12)}$$

Using Eq. (A11) and noting $\mathbf{n}\cdot\hat{\mathbf{x}} = \mathbf{n}\cdot\hat{\boldsymbol{\rho}}\cos\phi$, we have

$$\begin{aligned}\alpha_{\perp} &= \int_{S_p} \mathrm{d}s\rho\cos^2\phi\mathbf{n}\cdot(-\nabla v/\Omega + \hat{\rho}) \\ &= -\int_{S_p} \mathrm{d}s\rho\cos^2\phi\mathbf{n}\cdot\nabla(v/\rho\Omega) \\ &= -\frac{1}{2}\int_{S_p} \mathrm{d}s\rho\mathbf{n}\cdot\nabla(v/\rho\Omega) = \frac{\zeta_{\parallel}}{2\eta_0}\end{aligned}$$

which is just Eq. (10).

References

[1] I.D. Kuntz, W. Kauzman, Hydration of proteins and polypeptides, Adv. Protein Chem. 28 (1974) 239–345.

[2] P.G. Squire, M.E. Himmel, Hydrodynamics and protein hydration, Arch. Biochem. Biophys. 196 (1979) 165–177.

[3] S.E. Harding, A general method for modeling macromolecular shape in solution. A graphical (II-G) intersection procedure for triaxial ellipsoids. Biophys. J. 51 (1987) 673–680.

[4] J. Muller, Prediction of the rotational diffusion behavior of biopolymers on the basis of their solution or crystal structure, Biopolymers 31 (1991) 149–160.

[5] D.C. Teller, E. Swanson, C. de Haen, The translational friction coefficients of proteins, Methods Enzymol. 61 (1979) 103–124.

[6] D. Brune, S. Kim, Predicting protein diffusion coefficients, Proc. Natl. Acad. Sci. USA 90 (1993) 3835–3939.

[7] H.-X. Zhou, Calculation of translational friction and intrinsic viscosity. II. Application to globular proteins, Biophys. J. 69 (1995) 2298–2303.

[8] J. Garcia de la Torre, M.L. Huerta, B. Carrasco, Calculation of hydrodynamic properties of globular proteins from their atomic-level structure, Biophys. J. 78 (2000) 719–730.

[9] L. Esposito, L. Vitagliao, F. Sica, G.S.A. Zagari, L. Mazzarella, The ultrahigh resolution crystal structure of ribonuclease A containing an isoaspartyl residue: Hydration and sterochemical analysis, J. Mol. Biol. 297 (2000) 713–732.

[10] I.D. Kuntz, Hydration of macromolecules. III. Hydration of polypeptides, J. Am. Chem. Soc. 93 (1971) 514–516.

[11] P.-H. Yang, J.A. Rupley, Protein–water interactions. Heat capacity of the lysozyme–water system, Biochemistry 18 (1979) 2654–2661.

[12] G. Careri, A. Giansanti, E. Gratton, Lysozyme film hydration events: An IR and gravimetric study, Biopolymers 18 (1979) 1187–1203.

[13] G. Careri, E. Gratton, P.-H. Yang, J.A. Rupley, Correlation of IR spectroscopic, heat capacity, diamagnetic susceptibility and enzymatic measurements on lysozyme powder, Nature 284 (1980) 572–573.

[14] J.A. Rupley, E. Gratton, G. Careri, Water and globular proteins, Trends Biol. Sci. 8 (1983) 18–22.

[15] P.J. Steinbach, B.R. Brooks, Protein hydration elucidated by molecular dynamics simulation, Proc. Natl. Acad. Sci. USA 90 (1993) 9135–9139.

[16] H.-X. Zhou, Calculation of translational friction and intrinsic viscosity. I. General formulation for arbitrarily shaped particles, Biophys. J. 69 (1985) 2286–2297.

[17] S.C. Sahu, A. Bhuyan, A. Majumdar, J.B. Udgaonkar, Backbone dynamics of barstar: A ^{15}N NMR relaxation study, Proteins 41 (2000) 460–474.

[18] J. Ye, K.L. Mayer, M. Stone, Backbone dynamics of the human CC-chemokine eotaxin, J. Biomol. NMR 15 (1999) 115–124.

[19] S.M. Gagne, S. Tsuda, L. Spyracopoulos, L.E. Kay, B. Sykes, Backbone and methyl dynamics of the regulatory domain of troponin C: Anisotropic rotational diffusion and contribution of conformational entropy to calcium affinity, J. Mol. Biol. 278 (1998) 667–686.

[20] N. Tjandra, S.E. Feller, R.W. Pastor, A. Bax, Rotational diffusion anisotropy of human ubiquitin from ^{15}N NMR relaxation, J. Am. Chem. Sic. 117 (1995) 12562–12566.

[21] P. Luginbuhl, K.V. Pervushin, H. Iwai, K. Wuthrich, Anisotropic molecular rotational diffusion in ^{15}N spin relaxation studies of protein mobility, Biochemistry 36 (1997) 7305–7312.

[22] S. Yao, D.K. Smith, M. Hinds, J.-G. Zhang, N.A. Nicola, R.S. Norton, Backbone dynamics measurements on leukemia inhibitory factor, a rigid four-helical bundle cytokine, Protein Sci. 9 (2000) 671–782.

[23] R. Campos-Oliva, M.F. Summers, Backbone dynamics of the N-terminal domain of the HIV-1 capsid proteins and comparison with G94D mutant conferring cyclosporin resistance/dependence, Biochemistry 38 (1999) 10262–10271.

[24] K. Kloiber, R. Weiskirchen, B. Krautler, K. Bister, Mutational analysis and NMR spectroscopy of quail cysteine and glycine-rich protein CRP2 reveal an intrinsic segmental flexibility of LIM domains, J. Mol. Biol. 292 (1999) 893–908.

[25] L.D. Favro, Phys. Rev. 119 (1960) 53.

[26] T.F. Kumosinski, H. Pessen, Estimation of sedimentation coefficients of globular proteins: An application of

small-angle X-ray scattering, Arch. Biochem. Biophys. 219 (1982) 89–100.
[27] S. Krause, C.T. O'Konski, Electric properties of macromolecules. VIII. Kerr constants and rotational diffusion of some proteins in water and in glycerol–water solutions, Biopolymers 1 (1963) 503–515.
[28] A.J. Cross, G.R. Fleming, Influence of inhibitor binding on the internal motions of lysozyme, Biophys. J. 50 (1986) 507–512.
[29] K. Dill, A. Allerhand, Small errors in C–H bond lengths may cause large error in rotational correlation times determined from carbon-13 spin-lattice relaxation measurements, J. Am. Chem. Soc. 101 (1979) 4376–4378.
[30] S.B. Bubin, N.A. Clark, G.B. Benedek, Measurement of the rotational diffusion coefficient of lysozyme by depolarized light scattering: Configuration of lysozyme in solution, J. Chem. Phys. 54 (1971) 5158–5164.
[31] S.R. Anderson, M. Brunori, G. Weber, Fluorescence studies of Aplysia and sperm whale apomyoglobins, Biochemistry 9 (1970) 4723–4729.
[32] T. Tao, Time-dependent fluorescence depolarization and Brownian rotational motion coefficients of macromolecules, Biopolymers 8 (1969) 609–632.
[33] L. Stryer, The interaction of a naphthalene dye with apomyoglobin and apohemoglobin. A fluorescence probe of non-polar binding sites, J. Mol. Biol. 13 (1965) 482–495.
[34] L. Stryer, Fluorescence spectroscopy of proteins, Science 162 (1968) 526–533.
[35] G. Otting, E. Liepinsh, K. Wuthrich, Protein hydration in aqueous solution, Science 254 (1991) 974–980.
[36] L.D. Landau, E.M. Lifshiz, Fluid Mechanics, 2nd ed., Butterwork-Heinemann, Oxford, 1987.
[37] G.B. Jeffrey, On the steady rotation of a solid of revolution in a viscous fluid, Proc. Lond. Math. Sic. 14 (1915) 327–338.
[38] P.C. Chan, R.J. Leu, N.H. Zargar, On the solution for the rotational motion of an axisymmetric rigid body at low Reynolds number with application to an finite cylinder, Chem. Eng. Commun. 49 (1986) 145–163.